

INTEGRATION OF DETECTOR INTO INTERACTION REGION AT MEIC*

V.S. Morozov[#], R. Ent, P. Nadel-Turonski, Jefferson Lab, Newport News, VA
 C.E. Hyde, Old Dominion University, Norfolk, VA

Abstract

The Jefferson Lab’s Medium-energy Electron Ion Collider (MEIC) is proposed as a next-generation facility for the study of strong interaction (QCD). Accessing the relevant physics requires a full-acceptance detector with a dedicated small-angle high-resolution detection system capable of covering a wide range of momenta (and charge-to-mass ratios) with respect to the original ion beam. We present a design of such a detection system integrated into the collider’s interaction region, in which full acceptance is attained by letting small-angle collision products pass through the nearest elements of the machine final-focusing system for further detection. The proposed design is consistent with the current collider optics and demonstrates an excellent performance in terms of detector acceptance and resolution.

INTRODUCTION

The MEIC [1] is a highly asymmetric collider with the ion energy (20-100 GeV for protons or 12-40 GeV/u for ions) an order of magnitude greater than that of the electrons (3-11 GeV). From simple kinematics, the reaction products are biased towards small angles around the original ion beam. In particular, an essential part of the new physics at the MEIC [2] requires detection of small-angle products, such as the recoiling target baryon (3D structure of the nucleon), hadrons produced from its breakup (target fragmentation), or all the possible remnants produced when using nuclear targets (including the tagging of spectator protons in polarized deuterium), over a wide range of momenta (and charge-to-mass ratios) with respect to the original ion beam.

From machine design and luminosity considerations, it is not desirable to leave a very large detector space free of beam focusing elements to allow the small-angle products to accumulate sufficient transverse separation from the incident beams. The solution is to let the small-angle particles pass through the nearest elements of the machine

final-focusing system, which simultaneously perform the function of angle and momentum analyzer for the small-angle reaction products. A significant challenge of this approach is that it has to consistently reconcile often-contradictory detector and machine optics requirements.

DETECTOR MODEL

Figure 1 shows a schematic layout of one of the MEIC interaction regions containing a full-acceptance detector [2]. The electron and ion beams cross at a relatively large angle of 50 mrad, which greatly improves the momentum resolution for hadrons detected within a few degrees of the ion beam direction, and provides fast separation of the two beams thus eliminating parasitic bunch collisions and allowing one to move the final focusing elements closer to the interaction point (IP). The electron beam is aligned with the detector axis to avoid generation of synchrotron radiation.

The central detector is built around a 5 m long solenoid extending 3 m on the outgoing ion side and 2 m on the opposite side. The solenoid field is adjustable independently of the beam energies in order to optimize the detection for various processes. The maximum field is expected to be between 2 and 4 T. The solenoid is surrounded by 2 m long detector end caps.

Electrons scattered at small angles ($<1^\circ$) are detected in a low- Q^2 tagger consisting of a large-aperture electron final-focusing block (FFB) and a horizontal dipole magnet followed by a 5-10 m long drift space for momentum analysis.

In addition to benefiting from the large crossing angle in the solenoid, charged hadrons with scattering angles below $3\text{-}5^\circ$ with respect to the ion beam will pass through a large-aperture 2 Tm dipole (Dipole 1) located before the ion FFB. The dipole is 1 m long and is followed by 1 m of drift space and detectors. Particles at very small angles ($<0.5^\circ$) will pass through the ion FFB quads and then, after a few meters of a drift space, through a 20 Tm dipole (Dipole 2) for momentum analysis. Various detector elements are placed in the space between the final focus and Dipole 2 as well as beyond the dipole to provide complete angular and momentum coverage.

* Notice: Authored by Jefferson Science Associates, LLC under U.S. DOE Contract No. DE-AC05-06OR23177. The U.S. Government retains a non-exclusive, paid-up, irrevocable, world-wide license to publish or reproduce this manuscript for U.S. Government purposes.

[#] morozov@jlab.org

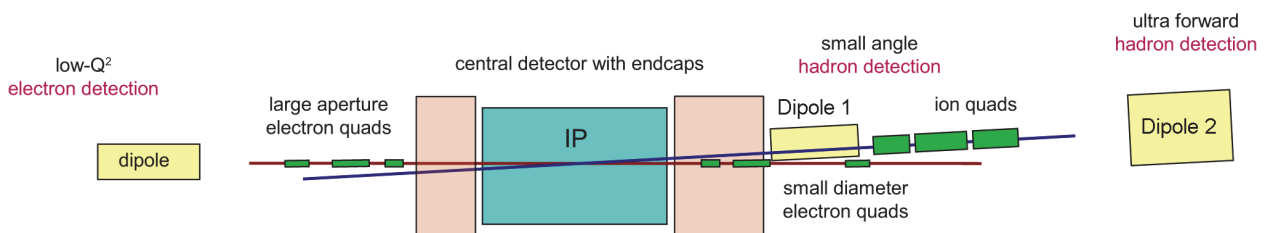


Figure 1: Schematic layout of the MEIC full-acceptance detector region.

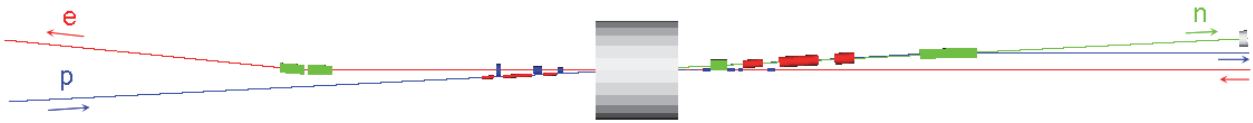


Figure 2: Scaled G4beamline/GEANT4 3D model of the MEIC full-acceptance detector region.

Following the above guidelines, we developed a complete G4beamline/GEANT4 3D model [3] of the detector region design shown in Fig. 1. A top view of the model is shown in Fig. 2. Special attention was paid to sizes and positions of the detector region elements to avoid them interfering with each other and with the detector functionality. To provide a realistic solenoid field for particle tracking, the solenoid was modeled as a set of many infinitely-thin current sheets evenly spread in the radial direction with the solenoid fringe field penetrating into the nearby magnets. The remaining detector region elements, including dipoles and quadrupoles, were modeled as hard-edge pure multipoles. Below we will focus our discussion on the design aspects related to detection of the small-angle forward-scattered hadrons, which is perhaps the most demanding part of the design.

FORWARD HADRON DETECTION

Ion Detector Region Optics

Figure 3 shows a detector-optimized optics of the ion interaction region. The corresponding magnet parameters are listed in Table 1. The solenoid effect is not taken into account in Fig. 3; however, it is included in the detector region model used for the tracking studies presented below. Note that the optics in Fig. 3 is not symmetric. The upstream FFB is placed closer to the IP than the downstream one, which is beneficial in reducing the upstream FFB's β -functions and chromatic contribution. The field parameters of the upstream quads are very modest. Their apertures are determined by the beam size and are chosen to provide at least $\pm 10\sigma$ beam stay clear. Their outer sizes must be made as small as possible to minimize their interference with detection of the forward-scattered electrons.

The downstream FFB is preceded by the small spectrometer dipole (Dipole 1) and is located 7 m from the IP. To maximize its acceptance to the forward-scattered hadrons, it was designed so that the apertures of its quads become progressively larger (while remaining constant within each quad) with increasing distance from the IP. For maximum acceptance, the apertures (R_{inner}) must be made as large as possible. They are limited by the maximum pole-tip fields ($B_{pole-tip}$) and the field gradients ($\partial B_y/\partial x$) required at the top energy ($R_{inner} = B_{pole-tip}/\partial B_y/\partial x$).

The ion beam is focused downstream of the forward FFB. The beam reaches the focal point after passing through a 4 m drift, the large spectrometer dipole (Dipole 2) with a bending angle of 60 mrad, and a 16 m drift. Having a small beam size at the focal point lets one place the detectors closer to the beam center. In combination with ~ 1 m dispersion at that point, this

allows detection of particles with small momentum offsets $\Delta p/p$. In comparison with a scheme where the beam is parallel after the FFB, focusing the beam reduces the minimum detectable $\Delta p/p$ by a factor of 6 (for a particle that initially moves along the beam). Incorporating this detector-optimized optics into the collider ring lattice requires some modification of the current design [4]. However, this should not pose any conceptual problems, since the optimized optics is consistent with all of the present machine design concepts. Moreover, due to its smaller chromatic contribution, the chromaticity compensation task is simplified.

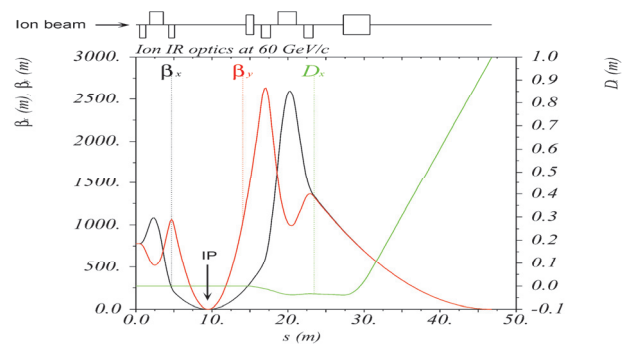


Figure 3: Ion interaction region optics.

Table 1: Parameters of the ion detector region magnets.

Magnet	$B_{pole-tip}$ (T)	$\partial B_y/\partial x$ (T/m)*	Length (m)	R_{inner} (cm)	L to IP (m)**
Upstream ion FFB					
Quad 1u	5.4	180.5	0.8	3	4.4
Quad 2u	3.4	85.7	1.8	4	5.9
Quad 3u	2.5	63.0	0.8	4	8.2
Downstream ion FFB					
Dipole 1	2	N/A	1	20	5
Quad 1d	9	89.0	1.2	10.1	7
Quad 2d	9	51.1	2.4	17.6	9.2
Quad 3d	7	35.7	1.2	19.6	12.6
Dipole 2	6	N/A	3.5	30	17.8

* maximum values corresponding to 100 GeV protons

** distance from the IP to the magnet side facing the IP

Detector Acceptance and Resolution

The forward ion FFB is designed so that its quads have about 0.7° polar angle aperture openings. This determines its acceptance to neutral reaction products. Charged particle trajectories, however, are affected by the FFB's quadrupole fields. Therefore, understanding the forward acceptance to different angles and momenta (or, equivalently, charge-to-mass ratios) requires particle tracking.

To study the forward hadron acceptance, we tracked multiple protons originating at the IP with different initial angles and momentum offsets with respect to a nominal 60 GeV/c proton beam. We determined which particles passed through the apertures of the forward ion quads. The solenoid field was 4 T at the center, the first spectrometer dipole field was 1.2 T, and the FFB quad gradients were adjusted to their 60 GeV/c values. The quads were modeled as cylinders with the inner radii given in Table 1. All particles that went outside the apertures anywhere inside the quads were considered lost. Figure 4 shows the result of tracking 10^4 protons with their momentum offsets $\Delta p/p$ uniformly distributed within ± 0.7 and their initial horizontal angles θ_x uniformly distributed within $\pm 1^\circ$ around a 60 GeV/c proton beam (all initial vertical angles were zero). The particles that clear the FFB are shown in blue. The black box indicates the phase space area of interest for detection. The acceptance for the most part covers and even exceeds that area assuming technically feasible maximum pole-tip fields of 7-9 T (see Table 1) at the top energy. Optimizing the forward FFB may further improve its acceptance.

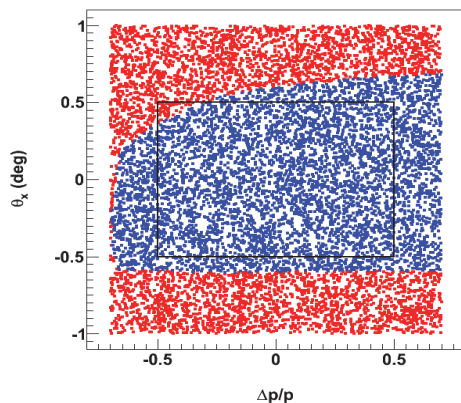


Figure 4: Acceptance (blue region) of the forward ion FFB in the horizontal plane.

Another importance characteristic of the detector performance is the detector resolution, i.e. the dependence of the particle's measured track on the initial parameters. We calculated the particle position at a few locations along the beam line as a function of its parameters at the IP. Figure 5 is an example of such a study showing the particle's horizontal position at the beam focal point 16 m downstream of Dipole 2 as a function of the particle's $\Delta p/p$ for a number of different initial horizontal θ_x and

vertical θ_y angles. The bottom graph in Fig. 5 is an expanded version of the top figure focusing on small values of $\Delta p/p$. The red band indicates the nominal $\pm 10\sigma$ beam stay-clear region, outside of which the particle can be detected. The points where the curves cross the red band boundaries determine the $\Delta p/p$ measurement limits, while the slopes of the curves determine the momentum measurement precision. The presented design demonstrates an excellent performance in terms of the detector acceptance and resolution and offers promising opportunities for nuclear physics studies.

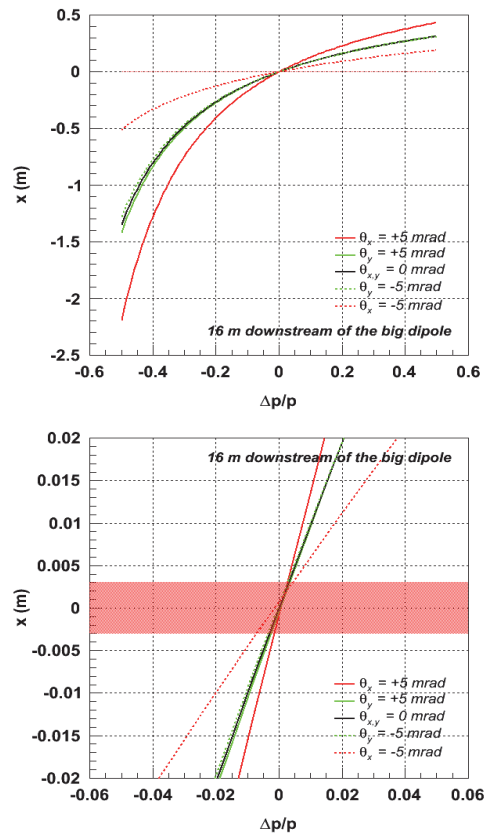


Figure 5: Detector momentum resolution 12 m downstream of the 2nd ion spectrometer dipole for a characteristic set of different initial angles. The bottom plot is an expanded version of the top figure. The red band is the nominal $\pm 10\sigma$ beam stay-clear region.

REFERENCES

- [1] Zeroth-Order Design Report for the Electron-Ion Collider at CEBAF, edited by Ya.S. Derbenev et al., <http://web.mit.edu/eicc/DOCUMENTS/ELIC-ZDR-20070118.pdf>
- [2] Gluons and the quark sea at high energies: distributions, polarization, tomography, arXiv:1108.1713v2 [nucl-th].
- [3] G4beamline, <http://g4beamline.muonsinc.com>
- [4] V.S. Morozov et al., in Proc. IPAC'11, THPZ017.